Structural Integrity of an Ablating Rocket Subjected to Axial Acceleration

GERALD H. LINDSEY* AND M. L. WILLIAMS†
California Institute of Technology, Pasadena, Calif.

One of the important design conditions for solid propellant rocket motors is that of inertia loading due to long term storage at 1 g, or acceleration in short time to high g. This paper investigates the structural integrity for inertia loading of a long, bonded, thick-walled cylinder, and includes the parametric considerations of rocket diameter $2b$, web fraction λ, inertia g-level n, and reduced burnout time t_f/a_T, as well as employing typical propellant properties and allowing for various burning rates of the eroding boundary. Finite end effect correction factors can be included from references already in the literature. By assuming a maximum shear strain failure criterion, a design envelope is obtained of $\rho g n b$ vs t_f/a_T, which expresses the interaction among the various parameters.

Introduction

ONE of the important design conditions for a solid propellant rocket motor concerns its structural integrity under inertia loading. Problems associated with spin stabilization, storage, maneuvering, wind shear, and acceleration fall into this category. Frequently a simultaneous consideration of the burning surface, which causes a change of the mass with time, compounds the problem. Until recently, the complexity of viscoelastic analysis for solid propellant grain materials has deterred quantitative attack upon the problem, particularly inasmuch as a completely adequate failure criterion has not been established. Nevertheless, present progress in material characterization, engineering analysis, and failure determination, as summarized by Williams,[1] is encouraging enough to undertake the quantitative evaluation of structural integrity for many combinations of configuration and loading.

The particular inertia problem to be discussed is a rather restricted and simple example of the more general one, which ordinarily occurs in practice. On the other hand, most of the controlling design factors are reflected in the idealized problem, and hence an important insight into the behavior of an accelerating rocket with ablation can be obtained. It is proposed to restrict our consideration to the problem of axial inertia alone, whether at rest as in a storage condition for long times, or in accelerated flight for short times. Furthermore a case-bonded, long circular port grain will be assumed, although the implications of these simplifying assumptions will be discussed.

An elastic analysis would indicate that there is no essential difference between a 1-g storage loading for long time and an n-g acceleration loading for short times, aside from the obvious magnitude factor due to the increased effective weight. However, because the grain material is viscoelastic, a time dependency arises due to the sensitivity of the material as it responds to different loading conditions. Furthermore, the failure mode itself is affected by the loading time and temperature, as is obvious in the failure of typical propellants at short as opposed to long loading times. The analysis will also include the effect of an ablating boundary, which allows for a decreasing weight with time. The (constant) burning rate of the propellant will therefore also enter as a design parameter. Finally, in order to illustrate how design envelopes may be constructed, a failure criterion will be assumed and representative results will be obtained showing how the design parameters of web fraction, burning rate, and inertia factors interact with the rocket size.

Background Studies

Notwithstanding the basic restriction in this paper to an infinite-length grain, it is appropriate to review some of the more general background material. There are basically two types of failure. The first mode is deformation critical, and leads to excessive slump in the grain and eventual port choking or deleterious effects on the burnout times. The second is stress or strain critical and is usually reflected in separation of the grain and case at the bonded interface.

Knauss[2] presented initial estimates of grain slump due to axial inertia for the two limits of the support condition: 1) a supported base that minimizes the criticalness of the stress at the expense of increasing the choking deformation(1), Fig. 1

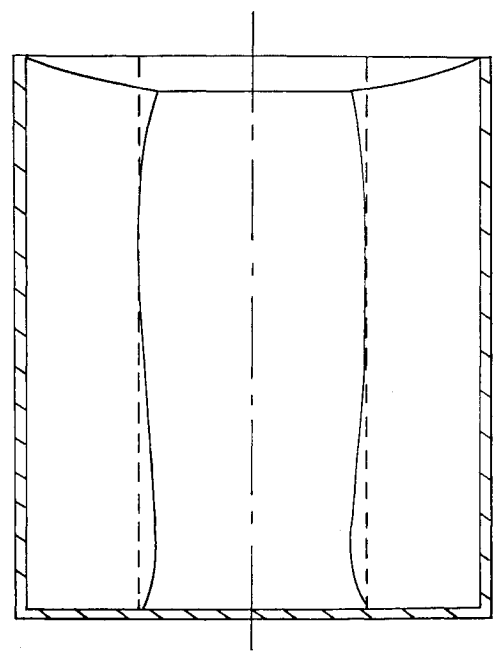

Fig. 1 Deformation of the internal boundary in the supported cylinder.[2]

Presented as Preprint 64-151 at the AIAA Solid Propellant Rocket Conference, Palo Alto, Calif., January 29–31, 1964. The work reported herein was supported in part under Research Grant No. NsG-172-60 from NASA and reported in the Graduate Aeronautical Laboratories, California Institute of Technology Rept. GALCIT SM 63-30.

* Research Assistant, Graduate Aeronautical Laboratories. Student Member AIAA.

† Professor of Aeronautics, Graduate Aeronautical Laboratories. Associate Fellow Member AIAA.

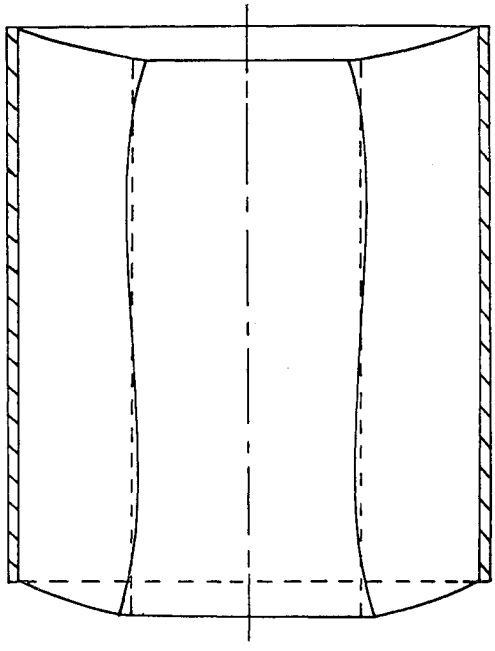

Fig. 2 Deformation of the internal boundary in the unsupported cylinder.[2]

and 2) a free, unsupported base for which the reverse is true (Fig. 2). The Knauss approximate analysis was based upon a minimum energy solution and has been superseded by the more comprehensive calculations of Parr[3] who obtained a digital numerical solution of the pertinent three-dimensional equations using Southwell stress functions.

For our present purpose, the essential feature of the analysis, as deduced from elementary considerations and amplified by the work of Knauss and Parr, is that the stress in the grain is proportional to $n\rho gb$, the strain to $n\rho gbD$, and the displacement to $n\rho gb^2D$, where ρg is the weight density of the propellant, b is the outside radius, and D is the compliance. For a step function loading, the time-dependent slump deformations may be predicted, without formal viscoelastic analysis, by using the creep compliance $D(t)$ as measured in a tensile test.[4]

A solution for the complications introduced by an ablating boundary was first given by Lee et al.[5] for a circular port grain, and extended for the similar problem of a sphere by Arenz and Williams.[6] The Lee-Radok solution emphasized the limitations of the Laplace transform technique when applied to this type of problem, and incorporated a simple three-element model approximation to the viscoelastic behavior.

For this particular case of axial acceleration, it so happens that the stress fields due to inertia and pressurization are essentially independent. Furthermore, for a known burning rate and acceleration trace, a viscoelastic analysis for internal port deformations and interface shear stress and strain can be rather easily completed. In fact, it can be done for realistic broad band material characterization[7] without having to simplify the viscoelastic model to three or four elements for computational simplicity.

Formulation of the Problem

The geometry to be considered is an infinitely long cylinder having a circular port of ablating radius $a(t)$, and an outer radius b at which the rocket grain is bonded to a rigid case. The radial coordinate is r, and the axial coordinate is z in the direction of the acceleration $gn(t)$. For these conditions of axial symmetry of the geometry and body force loading in the z direction $\rho gn(t)$, the three equations of equilibrium reduce simply‡ to

$$(1/r)(\partial/\partial r)(r\tau_{rz}) + \rho gn(t) = 0 \tag{1}$$

Because the shear stress is thus statically determinate, it can be found by quadrature for arbitrary $n(t)$ with relative ease.§ The boundary conditions appropriate to this analysis require that

$$\tau_{rz}[a(t), t] = 0 \tag{2}$$

$$u(b, t) = w(b, t) = 0 \tag{3}$$

where u and w are the radial and axial displacements, respectively.

As may be verified by direct substitution, the solution to (1) is

$$\tau_{rz}(r, t) = -[\rho gn(t)/2]\{[c(t)/r] + r\} \tag{4}$$

where $c(t)$ is an unknown function of time. From the boundary condition (2), it is found that $c(t) = -a^2(t)$ for $0 \leq t \leq t_f$, where t_f designates burnout. The complete solution is found by using the hereditary integral material characterization to first find the shear strain as

$$\gamma_{rz}(r, t) = J_{\text{crp}}(0)\tau_{rz}(t) + \int_0^t \tau_{rz}(r, t - \xi)\left[\partial J_{\text{crp}}\frac{(\xi)}{\partial \xi}\right] d\xi \tag{5}$$

Furthermore, noting that for the infinite-length grain

$$\gamma_{rz}(r, t) = \partial w/\partial r \tag{6}$$

an integration of (5) using (4) and boundary condition (3) gives the displacement as

$$w(r, t) = \frac{J_g\rho gn(t)}{2}\left[-a^2(t)\ln\frac{b}{r} + \frac{b^2 - r^2}{2}\right] + \int_0^t \frac{\rho gn(t - \xi)}{2}\left[\frac{b^2 - r^2}{2} - a^2(t - \xi)\ln\frac{b}{r}\right]\frac{\partial J_{\text{crp}}(\xi)}{\partial \xi} d\xi \tag{7}$$

and the problem is formally solved.

Typical Physical Problem

In order to make the ensuing discussion more meaningful, we shall utilize specific, reasonable functions for the acceleration and burning rate. The acceleration will be conservatively approximated as a Heaviside step function, since the actual trace will lead to a less severe loading, and the burning rate will be assumed constant. It may be noted, however, that virtually any reasonable or actual time-dependent function may be introduced without unduly complicating the analysis. Furthermore, for an incompressible material the shear creep compliance $J_{\text{crp}}(t)$ equals three times the tensile creep compliance $D_{\text{crp}}(t)$, which is itself approximately equal to the inverse tensile relaxation modulus,[1] namely,

$$J_{\text{crp}}(t) = 3D_{\text{crp}}(t) \doteq 3E_{\text{rel}}^{-1}(t) \tag{8}$$

Upon introducing these assumptions and defining a_0 as the initial internal radius and b as the outside radius, we have

$$n(t) = n_0 \tag{9}$$

$$a(t) = a_0 + (b - a_0)(t/t_f) \equiv a_0 + mt \tag{10}$$

which gives the shear stress explicitly as

$$\tau_{rz}(r, t) = \frac{\rho gn_0}{2}\left[\frac{(a_0 + mt)^2}{r} - r\right] \tag{11}$$

where the independence of material properties must be noted.

‡ The radial equation of equilibrium is satisfied by $\sigma_r = \sigma_\theta = 0$ for a rigid case, and for the infinite length grain $\sigma_z = 0$.

§ A direct application of the Alfrey viscoelastic analogy is inappropriate, because at best it leads to artificial restrictions upon the Laplace transformed equation and ablating boundary.

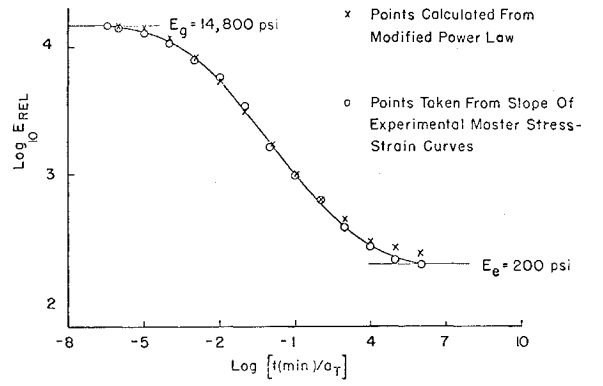

Fig. 3a Modified power law representation of relaxation modulus for HC propellant[7] $a_T = 1$ at $T = -30°C$ for Williams Landel Ferry (WLF) time-temperature shift.[1]

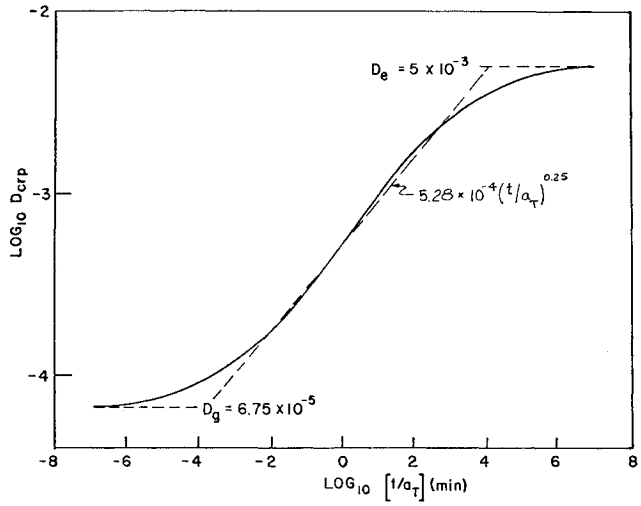

Fig. 3b Creep compliance for HC propellant, using Williams Landel Ferry(WLF) time-temperature shift[1] with $a_T = 1$ at $T = -30°C$, approximated from the relation $D_{crp} = [E_{rel}]^{-1}$ using Fig. 3a data for HC propellant.

Substitution into (5) gives the shear strain as

$$\gamma_{rz}(r, t) = -\frac{\rho g n_0 r}{2}\left\{\left[1 - \frac{1}{(r/a_0)^2}\right]J^{(0)}(t) - \frac{2(m/a_0)}{(r/a_0)^2}J^{(1)}(t) - \frac{2(m/a_0)^2}{(r/a_0)^2}J^{(2)}(t)\right\} \quad (12)$$

where the functions $J^{(s)}(t)$, independent of geometric configuration and a function only of the material properties of the propellant, are defined as

$$J^{(s+1)}(t) = \int_0^t J^{(s)}(\xi)d\xi \qquad J^{(0)}(t) \equiv J_{crp}(t) \quad (13)$$

and are to be interpreted physically as repeated integrations of the compliance curve. Note also that in view of (10), the burning rate parameter can be replaced by the port size factor and burnout time, i.e., $m/a_0 = (\lambda - 1)/t_f$.

With these substitutions, and evaluating the strain for the critical position $r = b$, one finds

$$\gamma_{rz}(b, t) = -\frac{\rho g n_0 b}{2}\frac{\lambda^2 - 1}{\lambda^2}\left\{J_{crp}(t) - \frac{2}{\lambda + 1}\left(\frac{t}{t_f}\right)\times\left[\frac{J^{(1)}(t)}{t}\right] - \frac{2(\lambda - 1)}{\lambda + 1}\left(\frac{t}{t_f}\right)^2\left[\frac{J^{(2)}(t)}{t^2}\right]\right\} \quad (14)$$

The terms in braces emphasize the average character of the area integrals up to time t. Note that if the burnout time

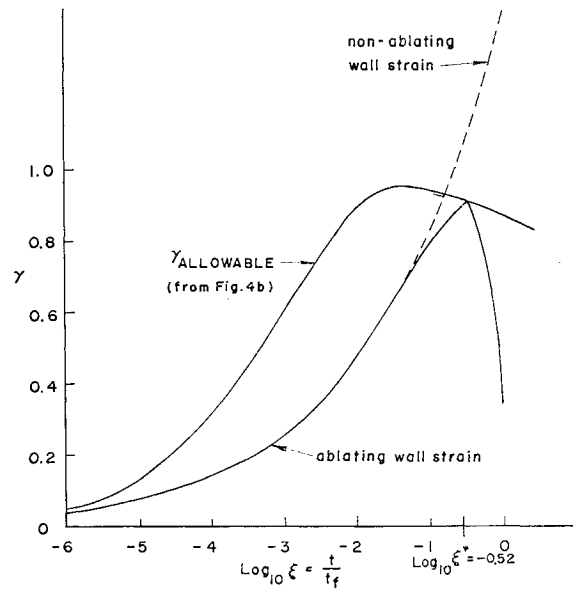

Fig. 4 Failure strain threshold ($\xi = \xi^*$) for a typical design configuration; $\lambda = 2$, $t_f/a_T = 1$, $\rho g n_0 b D_0 = 1$.

is infinite, i.e., no burning, the usual nonablating elastic solution due to the first term is recovered; the second and third terms are subtractive, illustrating the reduced shear strain at the wall as the propellant burns.

It remains to examine more specifically the behavior of the functions $J^{(s)}(t)$ inasmuch as they indicate the influence of the material. A study of them permits one to prescribe those mechanical properties required to achieve the design objective. The calculation of $J^{(s)}(t)$ is straightforward for any given propellant and may be performed using numerical integration of the experimental data directly, or incorporating an analytical representation of the data, as for example a collocation procedure and then quadrature. For the present purpose, however, it suffices to illustrate the point to be made by an approximate integration of a power law fit of the data.

Assume then that the tensile compliance data for a typical propellant, using (8), can be satisfactorily approximated by Eqs. (15) (Figs. 3a and 3b), where the reduced time variable is used to account for temperature effects:

$$D_{crp}(t) = D_g \qquad 0 \le t < t_g \quad (15a)$$
$$= D_0(t/a_T)^k \qquad t_g \le t \le t_e \quad (15b)$$
$$= D_e \qquad t > t_e \quad (15c)$$

As a result of the logarithmic time scale over which the compliance ranges, it develops that, except for minor discrepancies for times within one decade of t_g and t_e, the integrals in (14) can, for our purposes, be satisfactorily approximated and lead to the strain expressions as

$$\gamma_{rz}(b, t) = \frac{-3\rho g n_0 b}{2}\frac{\lambda^2 - 1}{\lambda^2}D_g\left\{1 - \frac{2}{\lambda + 1}\left(\frac{t}{t_f}\right) - \frac{\lambda - 1}{\lambda + 1}\left(\frac{t}{t_f}\right)\right\} \qquad t \le t_g \quad (16a)$$

$$\gamma_{rz} = \frac{-3\rho g n_0 b}{2}\frac{\lambda^2 - 1}{\lambda^2}D_0(t/a_T)^k\left\{1 - \frac{1}{k + 1}\frac{2}{\lambda + 1}\times\left(\frac{t}{t_f}\right) - \frac{2}{(k + 1)(k + 2)}\frac{\lambda - 1}{\lambda + 1}\left(\frac{t}{t_f}\right)^2\right\} \qquad t_g < t \le t_e \quad (16b)$$

$$\gamma_{rz} = \frac{-3\rho g n_0 b}{2}\frac{\lambda^2 - 1}{\lambda^2}D_e\left\{1 - \frac{2}{\lambda + 1}\left(\frac{t}{t_f}\right) - \frac{\lambda - 1}{\lambda + 1}\left(\frac{t}{t_f}\right)^2\right\} \qquad t > t_e \quad (16c)$$

In this form it is seen that the effect of ablation is reflected in the bracketed terms, which themselves are not functions of the time-temperature parameter a_T. The bracketed terms are essentially the same for all time ranges because $\frac{1}{4} \leq m \leq \frac{1}{2}$ for most propellants. Qualitatively, the ablation factor becomes nearly zero close to burnout and, by virtue of k and λ always being positive, the strain at the wall, while reducing due to ablation, does not reverse sign. From the practical standpoint, burnout will usually occur in the transition region $t_q < t \leq t_e$, and there will be a maximum strain at $t = t^*$ such that

$$\xi^* \equiv t^*/t_f = [2(\lambda - 1)]^{-1}\{[(k+1)^2 + 2k(k+1)(\lambda^2 - 1)]^{1/2} - (k+1)\} \quad (17a)$$

$$\gamma_{rz}(b, \xi^*) = \frac{-3\rho g n_0 b}{2} \frac{(\lambda^2 - 1)}{\lambda^2} D_0 \xi^{*k} \left(\frac{t_f}{a_T}\right)^k K^*(\lambda, \xi^*) \quad (17b)$$

where the bracketed term is denoted by $K(\lambda, \xi)$. The strain history for a typical configuration is indicated in Fig. 4.

Failure Analysis

Having completed a viscoelastic strain analysis, a strength analysis must be undertaken in order to assess the structural integrity. For illustrative purposes, the data of Kruse[7] for the material representation and failure characteristics of a typical propellant can be introduced (Figs. 5a and 5b). Note that the strain at break has been replotted in Fig. 6 in the equivalent form of strain vs time to failure in order to interpret the data more easily later.

Whereas in normal engineering materials failure will occur at some particular ultimate value of stress or strain, viscoelastic materials are quite rate and temperature sensitive. Thus the stress or strain at which failure occurs will depend upon the strain rate to which the material has been subjected. Moreover, as in most situations where the strain rate varies with time, failure will also depend upon strain rate history.

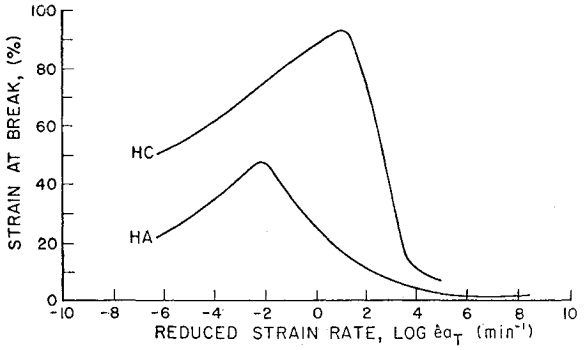

Fig. 5a Variation of strain at break with reduced strain rate.

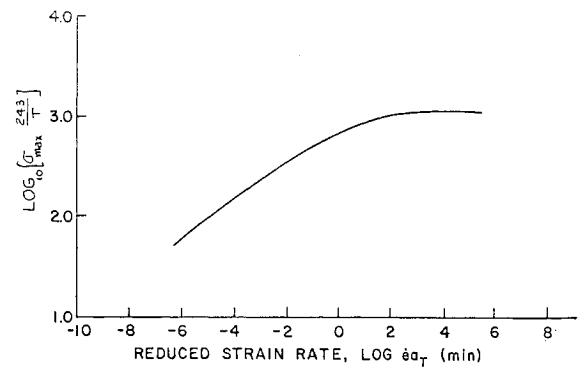

Fig. 5b Variation of tensile strength with reduced strain rate.

Unfortunately most failure testing has been conducted at constant strain rates to failure, as illustrated by Kruse's[7] data for tensile specimens. A bridge between variable and constant strain rate history is required, and for this purpose Williams[8] has suggested a cumulative damage concept pending experimental evidence to the contrary. On the other hand, an even simpler approach, particularly suitable for illustrative purposes, is to use merely the average strain rate $\bar{\dot{\gamma}}$ to the time in question. Physically it would be assumed that failure following a variable strain rate would occur at the same time as if the strain rate history were imposed at a constant rate equal to the average of the variable strain rate up to the time of failure. Thus

$$R \equiv \bar{\dot{\gamma}} = \frac{1}{t}\int_0^t \frac{\partial \gamma}{\partial t}\, dt = \frac{\gamma(t)}{t} \qquad \gamma(0) = 0 \quad (18)$$

The final assumption necessary to complete the failure analysis is one associating tensile and shear failure, required because of the lack of experimental shear data. In order to demonstrate the method of analysis, it has been arbitrarily assumed that

$$\gamma_{\max} = \epsilon_{\max} \text{ for } \dot{\gamma} = \dot{\epsilon} \quad (19)$$

Considering therefore that the actual strain rate history can be replaced by its average, using (18), the allowable strain to break γ_r at that average rate will, by hypothesis, be the same as that attained in the constant strain rate test, (19). Mechanistically, one can easily generate the parametric design curve by selecting a series of values $\bar{\dot{\gamma}}$ and reading off the corresponding series of allowable values γ_r from Fig. 5b. (The replot of Fig. 5b shown in Fig. 6 is often useful.) Then the division of one by the other gives the associated series of values of time to break $t_r = \gamma_r/\bar{\dot{\gamma}}$. Finally, for a given configuration, i.e., λ, t_f, a_T, one solves for the design parameter $\rho g n_0 b$ from (16) evaluated at $t = t_r$. Figure 4 shows the time of failure t_r as the point of tangency between the actual and allowable strain history.¶

Repetitive calculations were conducted for various values of web fraction to give a complete parametric representation of the various design capabilities (Fig. 7). The capability at extreme reduced burnout times is indicated by the asymptotes, and the maximum performance near a temperature-reduced burnout time of $t_f a_T = 0.01$ is immediately evident. For completeness, a nonablating strain is presented for comparison. As can be readily seen, if ablation is not accounted

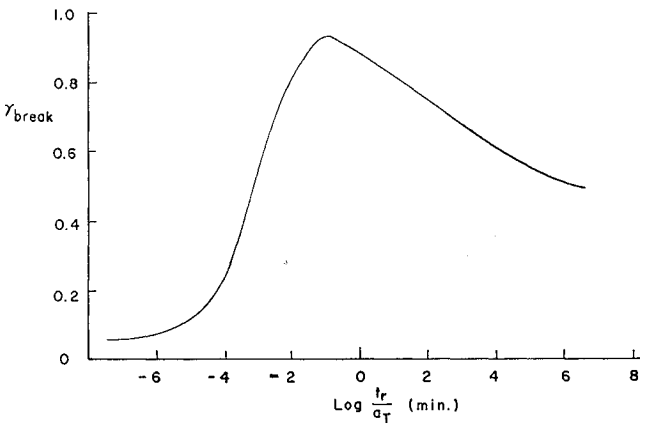

Fig. 6 Time to failure for constant strain rate HC propellant, replotted from Fig. 5b assuming $\gamma_{break} = \epsilon_{break}$.

¶ It is worth noting also that the time to break t_r is usually nearly coincident with the time for maximum strain t^* because of the sharply peaked character of the strain curve. Therefore, some computational simplicity can often be achieved by assuming them equal.

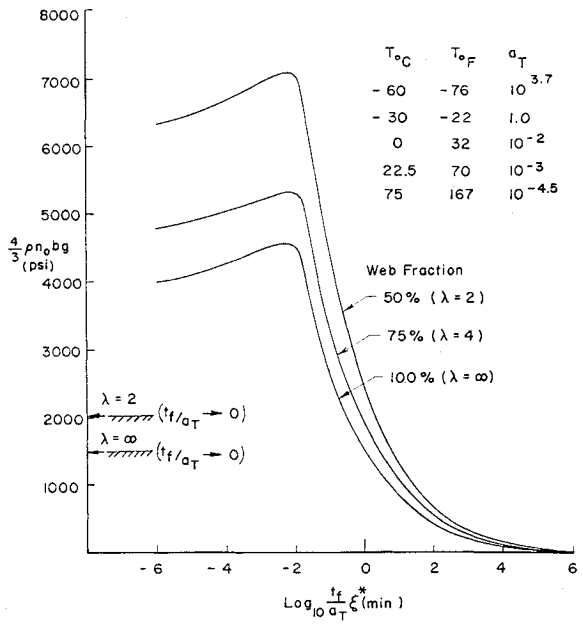

Fig. 7 Design curve for infinite length, rigidly encased, HC propellant tubular grain for step acceleration and constant burning rate.

for, an overly conservative design would result, significantly limiting the capability of the highly accelerated rockets.

Conclusions

The purpose of this paper has been to indicate the type of viscoelastic analysis which is involved in conducting a structural integrity study of an axially accelerated rocket. It is prudent, however, to emphasize certain shortcomings. Methods are available for analyzing the grain, but concurrently it should be evident that certain matters of an experimental nature, such as an applicable failure criterion and ultimate stress or strain data in shear, are still unresolved. As a result, the confidence limits on the resulting answer leave something to be desired. One might note, for example, that shear failure at the case was presumed to be independent of the radial and circumferential strain magnitudes that result from the pressurization loading. Indeed the introduction of multiaxial strains, which for this problem, even though small, would change the orientation and magnitude of principal strain, appears to reduce the amount of ultimate strain that the material can withstand. Experimental evidence along these lines has been reported by Ko[9] for biaxial fields and by Lindsey et al.[10] for the triaxial.

On the positive side, however, it is believed significant that practical methods are now available for the viscoelastic strain analysis, even if not for failure analysis, for this important design condition. In particular, the concentration effects due to star geometries can be treated by photoelastic methods[11] or conformal mapping[12] for the pressurization loading. Further, Parr[13] has shown how the accelerating star-grain concentration problem can be reduced to a simple Poisson equation adaptable to a digital computer. Finally the problem of a finite length grain can to a large extent also be considered solved by the parametric charts of Parr,[13] except for the continuing embarrassing difficulty of stress singularities[14] at the end of the grain which must still be treated by using an ample factor of safety applied to the average stress.

In conclusion, it is believed that the preliminary results, as reflected in Fig. 7, are reasonable and representative. It is imperative however that the accuracy of such predictions be reinforced by additional experimental work in failure conditions.

References

[1] Williams, M. L., "The structural analysis of viscoelastic materials," AIAA J. **2**, 785–808 (1964).

[2] Knauss, W. G., "Displacements in an axially accelerated solid propellant rocket grain," Graduate Aeronautical Labs., California Institute of Technology, GALCIT SM 61-21 (September 1961); also *20th Meeting Bulletin, JANAFAN Panel on Physical Properties of Solid Propellants*, Solid Propellant Information Agency, Johns Hopkins Univ. PP14u (1961), Vol. 1, pp. 175–186.

[3] Parr, C. H. and Gillis, G. F., "Deformation of case-bonded solid propellant grains under axial acceleration," AIAA Preprint 2750-63 (January 1963).

[4] Williams, M. L., Blatz, P. J., and Schapery, R. A., "Fundamental studies relating to systems analysis of solid propellants," Graduate Aeronautical Labs., California Institute of Technology, GALCIT SM 61-5 (February 1961); also Armed Services Technical Information Agency Rept. AD 256-905 (June 1961).

[5] Lee, E. H., Radok, J. R. M., and Woodward, W. B., "Stress analysis for linear viscoelastic materials," Trans. Soc. Rheol. **III**, 41–59 (1959).

[6] Arenz, R. J. and Williams, M. L., "The stresses in an elastically reinforced pressurized viscoelastic sphere with an eroding boundary." Graduate Aeronautical Labs., California Institute of Technology, GALCIT SM 61-20, (September 1961); also *20th Meeting Bulletin, JANAFAN Panel on Physical Properties of Solid Propellants*, Solid Propellant Information Agency, Johns Hopkins Univ. PP14u (1961), Vol. 1, pp. 143–153.

[7] Kruse, R. B., "The role of broad spectrum mechanical response studies in propellant evaluation," *20th Meeting Bulletin, JANAFAN Panel on Physical Properties of Solid Propellants*, Solid Propellant Information Agency, Johns Hopkins Univ. PP14u (1961), Vol. 1, pp. 395–409.

[8] Williams, M. L., "Mechanical properties and the design of solid propellant motors," *Solid Propellant Rocket Research* (Academic Press, Inc., New York, 1960), Vol. 1, pp. 67–100.

[9] Ko, W. L., "Application of finite elastic theory to the behavior of rubber-like materials," Ph.D. Dissertation, California Institute of Technology (June 1963); also Graduate Aeronautical Labs., California Institute of Technology, GALCIT SM 63-13 (June 1963).

[10] Lindsey, G. H., Schapery, R. A., Williams, M. L., and Zak, A. R., "The triaxial tension failure of viscoelastic materials," Graduate Aeronautical Labs., California Institute of Technology, GALCIT SM 63-6 (February 1963); also U.S. Air Force Aeronautical Research Lab. Rept. 63-152 (1963).

[11] Fourney, M. E. and Parmerter, R. R., "Photoelastic design data for pressure stresses in slotted rocket grains," AIAA J. **1**, 697–698 (1963).

[12] Wilson, H. B., "Conformal transformation of a solid propellant grain with a star shaped internal perforation onto an annulus," ARS J. **30**, 780–781 (1960).

[13] Parr, C. H., "Viscoelastic cylinders of complex cross section under axial acceleration loads," AIAA J. **1**, 2404–2406 (1963).

[14] Zak, A. R., "Stresses in the vicinity of boundary discontinuities in bodies of revolution," J. Appl. Mech. **31**, 150 (March 1964).